

1 *Mammalian orthoreovirus* infection is enhanced in cells pre-treated with sodium arsenite

2

3

4 Michael M. Lutz^a, Megan P. Worth^a, Meleana M. Hinchman^b, John S. L. Parker^b, Emily

5 D. Ledgerwood^{a#}

6

7

8 Department of Biological and Environmental Sciences, Le Moyne College, Syracuse,

9 New York, USA^a; Baker Institute for Animal Health, College of Veterinary Medicine,

10 Cornell University, Ithaca, New York, USA^b

11

12

13

14

15 Running Head: Sodium-arsenite pre-treatment enhances reovirus infectivity

16

17

18 [#]Corresponding author: Mailing address: Department of Biological and Environmental

19 Sciences, Le Moyne College, 1419 Salt Springs Rd, Syracuse, NY 13214. Phone: (315)

20 445-4237. Email: ledgered@lemoyne.edu

21

22

23

24 **ABSTRACT**

25 Following reovirus infection, cells activate stress responses that repress canonical
26 cellular translation as a mechanism to limit production of progeny virions. This includes
27 the formation of stress granules (SG) that sequester translationally-stalled cellular
28 transcripts, translation initiation factors, ribosomal proteins, and RNA binding proteins
29 until conditions improve and translation can resume. Work by others suggests that these
30 cellular stress responses, which are part of the integrated stress response, may benefit
31 rather than repress reovirus replication. In agreement with this, we report that stressing
32 cells prior to infection with sodium arsenite (SA), a robust inducer of SG and activator of
33 eIF2 α kinases, enhanced viral protein expression, percent infectivity and viral titer in SA-
34 treated cells compared to untreated cells. SA-mediated enhancement of reovirus
35 replication was not strain-specific, but was cell-type specific. While pre-treatment of cells
36 with SA offered the greatest enhancement, treatment of infected cultures as late as 4 h
37 post infection resulted in an increase in the percent of cells infected. SA activates the HRI
38 kinase, which phosphorylates eIF2 α and subsequently induces SG formation. Other
39 stresses, such as heat shock (HS) and osmotic shock also activate HRI. Heat shock of
40 cells prior to reovirus infection readily induced SG in greater than 85% of cells. Although
41 HS pre-treatment had no effect on the percentage of infected cells or viral yield, it did
42 enhance viral protein expression. These data suggest that SA pre-treatment perturbs the
43 cell in a way that is beneficial for reovirus and that neither HRI activation nor SG
44 induction is sufficient for reovirus infection enhancement.

45

46

47 **SIGNIFICANCE**

48 All viruses rely on the host translational machinery for the synthesis of viral
49 proteins. In response to viral infection, cells activate the integrated stress response
50 resulting in the phosphorylation of eIF2 α and translation shutoff. Despite this, reovirus
51 replicates to reduced titers in the absence of this response. In this work, we report that
52 sodium arsenite activation of the integrated stress response prior to virus inoculation
53 enhances virus infectivity, protein expression and titer. Together, these data suggest that
54 modulation of conserved cellular stress responses can alter reovirus replication.

55

56

57

58

59

60

61

62

63

64

65

66

67

68

69

70 INTRODUCTION

71 Acute viral infection induces stress within infected cells. The integrated stress
72 response (ISR) is activated in many cells during viral infection [1-3]. The ISR facilitates
73 cellular survival and a return to homeostasis, or initiates cell death signaling under
74 conditions of severe stress or when the initiating stressor is maintained [4]. Four distinct
75 stress kinases, can be activated in response to stress. Although, these kinases may have a
76 number of substrates, they all phosphorylate the alpha subunit of the eukaryotic
77 translation initiation factor 2 (eIF2 α) at serine position 51. When eIF2 α is
78 phosphorylated, eIF2B is unable to exchange GDP for GTP, preventing eIF2 interaction
79 with the Met-tRNA_i and translation initiation [4].

80 The ISR is activated in response to accumulation of phosphorylated eIF2 α . The
81 four cellular kinases that phosphorylate eIF2 α are heme-regulated eIF2 α kinase (HRI),
82 general control non-depressible 2 (GCN2), double-stranded RNA-dependent protein
83 kinase (PKR) and PKR-like ER kinase (PERK) [4]. Both cell intrinsic and extrinsic
84 stresses can activate these kinases: (i) HRI - heme-deprivation; (ii) GCN2 - amino acid
85 starvation; (iii) PKR - accumulation of double-stranded RNA (as can occur during viral
86 infection) and (iv) PERK - accumulation of unfolded proteins in the endoplasmic
87 reticulum (ER) [4]. However, redundancy does exist amongst the kinases. For example,
88 GCN2 is activated in response to ER stress in cells lacking PERK, and all four kinases
89 can be activated under oxidative stress [5-9].

90 When the alpha subunit of eIF2 is phosphorylated at position 51, the GDP-loaded
91 eIF2 entraps the limiting amounts of eIF2B leading to a rapid decrease in concentration
92 of functional eIF2.GTP.Met-tRNA_i ternary complexes. This results in reduced translation

93 initiation and inhibition of de novo protein synthesis [4]. In response to the inhibition of
94 translation initiation, stress granules (SG) form in the cytoplasm. SG assembly is
95 mediated by the RNA binding proteins T-cell antigen 1 (TIA-1), TIA-1 related protein
96 (TIAR) and the Ras-GAP SH3-binding protein 1 (G3BP1), and results in the
97 compartmentalization of translationally-stalled mRNA transcripts, RNA-binding proteins,
98 40S ribosomes, and translation initiation factors [10, 11]. SG are considered to be sites of
99 mRNA triage, protecting mRNA transcripts until a stress is alleviated and the cell returns
100 to homeostasis.

101 Many viruses prevent activation of the integrated stress response to maintain
102 protein translation and to ensure successful viral infection. To do this, viruses target the
103 initiating kinases and/or the downstream effector mechanisms of the ISR. Cells in which
104 the initiating kinases, such as PKR are inhibited or knocked out are often more
105 permissive for viral replication [12, 13]. However, not all viruses benefit from inhibition
106 of kinase activity and initiation of the ISR. A study examining the role of the PKR-eIF2
107 pathway during mammalian orthoreovirus (reovirus) infection found some strains had
108 reduced titers in PKR knockout murine embryonic fibroblasts (MEF) [14]. Follow-up
109 studies observed both increased ISR gene expression and reduced levels of the eIF2 α
110 kinase inhibitor P58^{IPK} in cells infected with reovirus strains known to robustly interfere
111 with host translation, and these strains replicated less efficiently in MEFs expressing a
112 non-phosphorylatable form of eIF2 α [15].

113 Reovirus infection also modulates stress granule formation that occurs
114 downstream of ISR activation [15, 16]. Early in infection, entering viral core particles
115 localize to stress granules that form within infected cells. However, within 4-6 h after

116 infection, the stress granules have disappeared and viral factories (VFs), the sites of
117 reovirus replication, transcription, translation and assembly, become prominent [16]. In
118 some reovirus-infected cells, the stress granule protein G3BP1 localizes to the margins of
119 the VFs, mediated by an interaction of G3BP1 with the non-structural viral protein σ NS
120 [17]; σ NS interacts with the nonstructural protein μ NS that forms the matrix of VFs [18].
121 Co-expression of σ NS and μ NS is sufficient to alter the localization of G3BP1 and
122 suppress stress granule induction [17]. The interplay between eIF2 α phosphorylation,
123 PKR activation, translational shutoff and G3BP1 induced SG formation is strain-
124 dependent, with SG formation negatively impacting some strains of reovirus [17].
125 Together, these studies suggest a unique role for the ISR during reovirus infection,
126 however the magnitude of this role remains to be elucidated. Most virological studies of
127 the ISR take two approaches: 1) understanding the impact of virus infection on stress
128 responses or 2) understanding how perturbing the ISR during infection affects the virus.
129 Given the previous observation that reovirus replicates to lower titers in cells with an
130 impaired ISR, we hypothesized that reovirus infection would be enhanced in cells in
131 which the ISR has been activated prior to infection. We found that reovirus infection was
132 more efficient (increased infectivity, protein expression, and replication) in cells in which
133 the ISR had been activated by pre-treatment with sodium arsenite prior to virus
134 adsorption. Sodium arsenite-induced enhancement of reovirus infection was observed in
135 all reovirus strains tested but was dependent on cell-type and the time of sodium-arsenite
136 addition. Enhancement of viral infectivity was only observed if sodium arsenite was
137 added to cells within 4 h of inoculation, with maximal enhancement if the addition
138 occurred prior to inoculation, suggesting a relationship between the ISR and early

139 replication events. Furthermore, not all activators of the ISR were equally beneficial as
140 heat shock prior to infection had no impact on viral replication. Taken together, these
141 data suggest a critical role for the ISR during reovirus infection and that activation of the
142 ISR prior to reovirus infection is beneficial in some cell-types.

143

144 **MATERIALS AND METHODS**

145 **Cells and reagents.** CV-1 (ATCC CCL-70) and HeLa cells were maintained in Eagles
146 minimum essential medium (MEM) (CellGro) containing 10% fetal bovine serum (FBS;
147 Hyclone), 100 mM sodium pyruvate (CellGro), and 200 mM L-glutamine (CellGro) at
148 37°C in the presence of 5% CO₂. L929 cells were maintained in MEM containing 8%
149 FBS and 200 mM L-glutamine at 37°C in the presence of 5% CO₂. Human Pancreatic
150 Ductal Epithelial (HPDE) cells (Kerafast H6c7) were maintained in keratinocyte SFM
151 (serum-free medium) supplemented with 25 mg bovine pituitary extract and 2.5 µg
152 human recombinant epidermal growth factor, both provided (Invitrogen) at 37°C in the
153 presence of 5% CO₂. Sodium arsenite was kindly donated by Dr. Shu-bing Qian (Cornell
154 University) and was used at a final concentration of 0.5 mM in all experiments.

155

156 **Viruses.** Reoviruses T1L and T3D laboratory stocks originated from the
157 T1/human/Ohio/Lang/1952 and T3/human/Ohio/Dearing/1955 isolates respectively [19].
158 The superscript T3D^N differentiates a clone obtained from M.L. Nibert (Harvard Medical
159 School) from T3D^C a clone obtained from L.W. Cashdollar (Medical College of
160 Wisconsin). The two clones have been shown to differ in M1 gene sequence and viral
161 factory morphology. All infections were performed with T3D^N (abbreviated T3D). The

162 prototype reovirus serotype 3 strain Abney (T3A) was a kind gift from Dr. Barbary
163 Sherry (North Carolina State University) and was plaque-purified and passaged twice on
164 L-cell monolayers to generate working stocks.

165

166 **Infections.** CV-1, L929, HeLa or HPDE cells were seeded in 24-well culture plates
167 containing 12 mm glass coverslips or 12-well culture plates the day before to give rise to
168 50 to 80% confluence prior to infection. Cells were infected with virus at the indicated
169 MOI for 1 h at room temperature (RT) in phosphate-buffered saline (PBS; pH 7.4),
170 supplemented with 2 mM MgCl₂, with rocking every 10 min. Following absorption, virus
171 was removed and cells were incubated in growth medium at 37°C and harvested at the
172 indicated time points.

173

174 **Antibodies.** The following commercial primary antibodies were used for
175 immunoblotting: mouse monoclonal anti-G3BP1 (2F3) antibody (H00010146-M01;
176 Novus Biologicals), mouse monoclonal anti-TIAR antibody (sc-398372; Santa Cruz
177 Biotechnology), and mouse monoclonal anti-alpha-tubulin antibody (NB100-690; Novus
178 Biologicals). Reovirus protein expression was assessed using a chicken polyclonal
179 antiserum against μ NS prepared against bacterially-expressed purified antigen by
180 Covance. Secondary antibodies used for immunoblotting were as follows: HRP Donkey
181 Anti-Mouse IgG (715-035-150; Jackson ImmunoResearch), and HRP Donkey Anti-
182 Chicken IgY (703-035-155; Jackson ImmunoResearch). Primary antibodies used for
183 immunofluorescence included: mouse monoclonal anti-G3BP1 (611126; BD
184 Biosciences), rabbit monoclonal anti-TIAR (8509S; Cell Signaling Technology), and

185 chicken polyclonal antiserum against μ NS to detect viral factories. Secondary Antibodies
186 used for immunofluorescence assays included Alexa Fluor 594 goat anti-chicken IgG,
187 Alexa Fluor 594 goat anti-rabbit IgG, Alexa Fluor 488 goat anti-mouse, and Alexa Fluor
188 488 goat anti-rabbit (ThermoFisher).

189

190 **Stress granule induction.** Stress granules were induced in cells using the following
191 mechanisms: 1) treatment with 0.5 mM sodium arsenite in normal growth media at 37°C
192 for 30 min prior to infection or 30 min prior to harvesting or 2) heat shock in normal
193 growth media in a pre-heated incubator at 44 °C for 45 min prior to infection or
194 harvesting. Cells were manually determined to contain stress granules if
195 immunofluorescence revealed a minimum of three granules co-staining for both TIAR
196 and G3BP.

197

198 **Immunofluorescence.** Cells were washed once with PBS supplemented with 2 mM
199 $MgCl_2$ and fixed at room temperature for 10 min with 4% paraformaldehyde in PBS.
200 Fixed cells were washed three times with PBS, permeabilized in 0.1% Triton X-100 in
201 PBS for 15 min and washed three times with PBS. Cells were blocked for 15 min in
202 staining buffer (SB; 0.05% saponin, 10mM glycine, 5% FBS, and PBS) and incubated
203 with primary antibodies diluted in SB for 1 h. Cells were then washed one time with PBS
204 before incubation with secondary antibodies diluted in SB for 1 h. Coverslips were
205 mounted onto glass slides with ProLong Gold Anti-Fade reagent with DAPI (4[prime],6-
206 diamidino-2-phenylindole; ThermoFisher). Images were obtained using an Olympus
207 BX60 inverted microscope equipped with phase and fluorescence optics. Images were

208 collected digitally with an Olympus DP74 color CMOS camera and cellSens Standard
209 Software (Olympus) and were processed and prepared for presentation using photoshop
210 (CC; Adobe) software.

211

212 **Immunoblot Assay.** Cells were lysed in PBS containing 0.5% NP40, 140 mM NaCl, 30
213 mM Tris-HCl (pH 7.4), and an EDTA-free protease inhibitor cocktail (04693159001;
214 Sigma Aldrich) for 30 min on ice. Cell lysates were resolved by SDS-PAGE and proteins
215 were detected using antibodies as described above. Images were collected using a C-Digit
216 digital scanner and Image Studio Digits software (Version 4, LiCor). When appropriate,
217 immunoblots were incubated in stripping buffer (200 mM glycine, 3.5 mM SDS, 1%
218 Tween 20, [pH 2.2]) and re-probed.

219

220 **Plaque Assay.** Cells were infected as above before washing with PBS supplemented with
221 2 mM MgCl₂ and incubated in growth medium at 37°C for the indicated times. Cells
222 were subjected to two freeze/thaw cycles prior to the determination of viral titer by the
223 standard reovirus plaque assay in L929 cells [20]. To determine the viral titer in PFU/ml,
224 the following equation was used: PFU/ml = number of plaques / (D × V) where D =
225 dilution factor and V = volume of diluted virus / well.

226

227 **RESULTS**

228 **Infection with reovirus induces stress granule formation.** Previous reports have
229 suggested that stress granules form following infection with reovirus, but reports are
230 conflicting as to the timing of stress granule presence in infected cells [15, 16] . To

231 evaluate this further, we first confirmed that stress granules could form in CV-1 cells by
232 treating uninfected cells with 0.5 mM sodium arsenite for 30 min. We then fixed and co-
233 immunostained for TIAR and G3BP, two RNA binding proteins required for stress
234 granule formation. We saw stress granules in ~91% of treated CV-1 cells, confirming that
235 these cells can form stress granules (Figure 1A, upper panels). We next infected CV-1
236 cells with reovirus at a multiplicity of infection (MOI) of 10 and fixed and
237 immunostained cells at the indicated times post-infection (p.i.) for the presence of stress
238 granules (TIAR), and viral factories (μ NS) (Figure 1A, lower panels). Stress granules
239 were absent in mock-infected cells and began appearing in infected cells around 2 h p.i.
240 We found that stress granule formation in reovirus-infected CV-1 cells peaked around 6 h
241 p.i. with 6.6% of cells containing stress granules. By 8 h p.i. the percentage of infected
242 cells containing stress granules had dropped to 3.1% and by 18 h p.i., the level was no
243 different from mock-infected cells (Figures 1A-B). A previous report showed that stress
244 granules were present in reovirus-infected human prostate carcinoma DU145 cells at 19.5
245 h post infection [15]. Although we did not see stress granules in CV-1 cells at late times
246 post-infection with reovirus at an MOI = 1, we found that G3BP and TIAR co-localized
247 at the periphery of viral factories at 24 h p.i. when cells were treated with 0.5 mM sodium
248 arsenite for 30 min immediately prior to harvest (Figure 1C). We occasionally saw a
249 similar phenotype at 24 h p.i. in infected cells not treated with sodium arsenite (Figure
250 1C). These findings are consistent with those of Choudhury et al. who found that G3BP
251 localizes to the viral factory periphery during reovirus infection [17]. While reovirus
252 appears to modulate the localization of stress granule proteins at late times post infection,
253 we observed only a modest increase in the expression level of stress granule protein

254 expression in infected cells as compared to mock that was independent of MOI (Figure
255 1D). Together, these data suggest that reovirus infection induces stress granules at early,
256 but not late times post-infection in CV-1 cells.

257

258 **Pre-treatment of cells with 0.5 mM sodium arsenite enhances reovirus infectivity.**

259 Following infection with reovirus, the viral protein μ NS orchestrates the formation of
260 viral factories, the sites of virus replication, assembly, and translation [21-23]. To
261 facilitate translation, cellular factors including eIF3, eIF4G and ribosomal subunits are
262 recruited to the viral factory [23]. Many of these initiation factors are similarly
263 compartmentalized within stress granules [24]. To date, most studies have focused on the
264 induction of stress granules in response to viral infection, or viral suppression of stress
265 granule formation during an infection. To our knowledge, no studies have been
266 performed to assess the impact of the presence of stress granules on reovirus infection.
267 To explore this, we first examined the effect of stress granule presence on viral protein
268 expression. CV-1 cells were either left untreated (-), or were treated with 0.5 mM sodium
269 arsenite for 30 min before infection at an MOI = 1 (pre) or 30 min before harvest (post).
270 Cell lysates were collected at 0, 6, 10, 18 and 24 h p.i. and the expression level of the
271 non-structural viral protein μ NS was determined (μ NS was first detectable by 10 h p.i.).
272 At 10, 18 and 24 h p.i., the expression levels of μ NS were consistently higher in cells pre-
273 treated with sodium arsenite when compared to untreated cells or cells treated with
274 sodium arsenite 30 min before harvest (Figure 2A).

275 As the viral protein μ NS is necessary for formation of viral factories during
276 reovirus infection, we next explored if the elevated μ NS expression was a consequence of

277 increased size of viral factories or increased numbers of infected cells [25]. We found
278 that in cells pre-treated with 0.5 mM sodium arsenite for 30 min prior to reovirus
279 infection, 67% of cells were infected (contained viral factories) at 18 h p.i., whereas only
280 33% of untreated cells were infected at 18 h p.i. (Figures 2B and C). We found similar
281 findings at 24 h p.i. (Figure 2C).

282 Given the increased percentage of infected cells in dishes pre-treated with sodium
283 arsenite, we tested if pre-treatment of cells with 0.5 mM sodium arsenite for 30 min
284 before reovirus infection enhanced viral yield. We found that pre-treatment with sodium
285 arsenite led to a modest but significant 2-3 fold increase in viral titer (PFU/ml) that was
286 independent of multiplicity of infection, but consistent with the increased numbers of
287 infected cells and the increased protein expression (Figure 2D). Together, these data
288 indicate that pre-treatment of cells with sodium arsenite enhances reovirus infectivity by
289 increasing the numbers of virus-permissive cells.

290

291 **SA-induced enhancement of reovirus infection is cell-type specific.** Previous reports
292 have suggested that reovirus-induced stress granule formation is cell-type specific [15,
293 16]. Therefore, we next sought to determine if the replication enhancement observed in
294 CV-1 cells was seen in other cell types. We assessed the effect of pre-treatment with 0.5
295 mM sodium arsenite on CV-1, HeLa, L929 murine fibroblasts, and human pancreatic
296 ductal epithelial (HPDE) cells on viral infectivity. In each cell line, a relative multiplicity
297 of infection was chosen such that 20-50% of cells were infected. Consistent with our
298 observations in CV-1 cells, pre-treatment with sodium arsenite in L929 and HPDE cells
299 resulted in a higher percentage of cells exhibiting viral factories than untreated cells

300 (Figure 3A). However, sodium arsenite pre-treatment did not increase the number of
301 infected HeLa cells (Figure 3A). These data indicate that activation of the stress response
302 pathways prior to infection through pre-treatment with sodium arsenite is beneficial in
303 some, but not all, cell types.

304

305 **SA-induced enhancement of reovirus infection is strain-independent.** The prototypic
306 reovirus strains Type 1 Lang (T1L), Type 2 Jones (T2J), Type 3 Abney (T3A), and Type
307 3 Dearing (T3D) differ in their capacity to induce host translational shutoff and to induce
308 eIF2 α phosphorylation [15, 26]. To determine if the benefit of pre-treatment with sodium
309 arsenite was reovirus strain specific, we infected CV-1 cells with T3D, T1L or T3A and
310 assessed the percentage of infected cells at 18 h p.i. compared to untreated cells. As
311 observed following infection with the T3D strain, pre-treatment with sodium arsenite
312 resulted in nearly a 2-fold increase in the percentage of T1L- and T3A-infected cells
313 (Figure 3B). Sodium arsenite pre-treatment in L929 cells infected with T3D, T1L or T3A
314 yielded similar results, however sodium arsenite pre-treatment had no effect on any strain
315 tested in HeLa cells (Supplemental Figure 1). These data suggest that reovirus strains
316 T3D, T3A and T1L benefit from pre-treatment with sodium arsenite prior to infection in
317 some cell types.

318

319 **Heat shock prior to infection enhances viral protein expression in T3D-infected L-**
320 **cells, but does not affect the percentage of infected cells or viral yield.** Of the four
321 stress-responsive kinases, sodium arsenite treatment activates HRI kinase. HRI is
322 activated in erythrocytes by reduced heme availability, but it is ubiquitously expressed in

323 many tissues and, when activated by sodium arsenite, phosphorylates eIF2 α and
324 subsequently induces stress granule formation [27]. HRI is the only stress kinase required
325 for translational inhibition in response to arsenite treatment in mouse embryonic
326 fibroblasts [27]. HRI kinase can also be activated by other cellular stresses including
327 osmotic stress and heat shock. To further assess if the enhanced reovirus infectivity
328 following sodium arsenite treatment was a consequence of HRI activation, we assessed
329 viral protein expression, the percentage of infected cells and viral yield in response to
330 heat shock. We used stress granule induction in response to heat shock as an indirect
331 measure of HRI activation (Figure 4A). Our attempts to induce stress granules in CV-1
332 cells with heat shock were only able to achieve no greater than 25% of cells containing
333 stress granules. Because of this, we assessed the effects of heat shock induction of stress
334 granules in L929 cells. Heat shock for 45 minutes at 44°C resulted in ~88% of L cells
335 containing stress granules (Figure 4A). Similar to our observations in CV-1 cells pre-
336 treated with sodium arsenite, viral protein expression was enhanced at 10 and 18 h p.i. in
337 L cells exposed to a 45 min heat shock prior to infection (Figure 4B). However, heat
338 shock activation had no impact on the percentage of infected cells or viral yield in L cells
339 (Figures 4C-E). These findings suggest that in L-cells, heat shock enhances protein
340 expression, but does not affect either the numbers of infected cells or the per cell yield of
341 virus. Although heat shock activates HRI kinase, its effect on cells differs from sodium
342 arsenite. Together, these data indicate that sodium arsenite pre-treatment perturbs the cell
343 in a way that is beneficial for reovirus compared to other activators of the HRI kinase.
344

345 **Addition of sodium arsenite prior to 4 hours enhances reovirus permissivity.**

346 Activation of the HRI kinase and eIF2 α phosphorylation suppress general host translation
347 [27]. We found that the enhancement of viral protein synthesis in cells pre-treated with
348 sodium arsenite treatment was not evident if cells were treated immediately prior to
349 harvest at 10, 18, or 24 h p.i. (Figure 2A). Given that viral protein expression, but not the
350 percentage of infected cells or viral yield, was enhanced by activation of the HRI kinase
351 using heat shock in L cells, we hypothesized that sodium arsenite treatment might
352 enhance viral translation at early times post infection. To test this, CV-1 cells were either
353 left untreated or were treated with 0.5 mM sodium arsenite at -0.5, 0, 1, 2, 4, 6, 8, or 10 h
354 p.i. We then assessed the percentage of infected cells at 18 h p.i.. Consistent with our
355 previous data, pre-treatment (-0.5 h p.i.) with sodium arsenite prior to inoculation with
356 virus resulted in an increase in the percentage of infected cells (Figures 5A-B). Although
357 pre-treatment had the greatest impact on reovirus permissivity, treatment with sodium
358 arsenite at 0, 1, 2 and 4 h p.i. resulted in an increased percentage of infected cells as
359 compared to untreated reovirus-infected cells (Figures 5A-B). Addition of sodium
360 arsenite at 6 h p.i. or later had no effect on the percentage of infected cells at 18 h p.i.
361 (Figures 5A-B). These data suggest that sodium arsenite is most beneficial when added
362 early during the viral life cycle.

363

364 **Preventing eIF2 α de-phosphorylation through the use of salubrinal has no effect on**

365 **reovirus replication.** Growth arrest and DNA damage protein-34 (GADD34) is
366 expressed in response to phosphorylation of eIF2 α as part of the ISR and is upregulated
367 in cells following infection with reovirus strains that induce host shut-off [15]. GADD34

368 is a protein phosphatase-interacting protein that, in conjunction with protein phosphatase
369 1 (PP1), acts to dephosphorylate eIF2 α at serine 51 during times of cellular stress [28].
370 Our findings thus far are consistent with previous reports suggesting that eIF2 α kinase
371 activation is beneficial to reovirus infection. We, therefore, hypothesized that reovirus
372 may be capable of viral protein synthesis in the face of enhanced eIF2 α phosphorylation.
373 We reasoned that inhibition of GADD34/PP1 dephosphorylation would enhance
374 phosphorylation of eIF2 α , but should have no effect on viral protein synthesis. We used a
375 selective inhibitor of GADD34, salubrinal, which prevents the activity of the
376 GADD34/PP1 complex without affecting the kinases that phosphorylate eIF2 α [29].
377 Immediately following adsorption of reovirus, CV-1 cells were treated with increasing
378 amounts of salubrinal and cells were harvested at 18 h p.i. to determine viral protein
379 expression (Figure 6A). Even at high concentrations, salubrinal had no impact on viral
380 protein expression, suggesting that reovirus tolerates the cellular antiviral activity of
381 eIF2 α phosphorylation. Given that sodium arsenite is a known inducer of eIF2 α
382 phosphorylation, we also tested the impact of adding salubrinal following reovirus
383 adsorption to sodium-arsenite pre-treated cells (Figure 6A). Again, we observed no
384 negative impact on viral protein expression when cells were pre-treated with sodium
385 arsenite prior to infection and then incubated in the presence of salubrinal for the duration
386 of infection (Figure 6A). Consistent with this, the percentage of virus infected cells was
387 unaffected by the addition of 50 mM salubrinal either in cells left untreated or cells pre-
388 treated with 0.5 mM sodium arsenite (Figures 6B-C). Together, these data suggest that
389 sustained eIF2 α -phosphorylation resulting from salubrinal treatment during reovirus
390 infection is not anti-viral.

391 **DISCUSSION**

392 In this report, we find that treatment of cells with sodium arsenite (SA), a potent
393 inducer of the integrated stress response (ISR) and eIF2 α phosphorylation, prior to
394 inoculation with reovirus is beneficial to the virus in a strain-independent but cell-type-
395 specific manner. SA treatment induces the formation of reactive oxygen species (ROS)
396 within cells. The increased intracellular ROS in turn lead to activation of HRI, which then
397 phosphorylates eIF2 α at serine residues 48 and 51 leading to general translation
398 repression and downstream activation of the integrated stress response. In order to mature
399 and become activated, HRI has to be in a complex with CDC37, PPP5C, and HSP90. In
400 addition to being activated by heme-deficiency, HRI is also activated by heat shock and
401 osmotic shock, but not by ER stress or by amino acid or serum starvation [7]. In contrast,
402 to the enhanced viral replication we saw following pre-treatment with SA, heat shock
403 (HS) pre-treatment did not enhance viral replication. Heat shock also activates HRI, but
404 to a qualitatively lower level than SA and with a different pattern of autophosphorylation
405 of HRI [7]. Why pre-stressing cells with SA, but not with heat shock, benefited viral
406 replication is unclear. It is possible that the kinetics, magnitude and timing of eIF2 α
407 phosphorylation following these different stressors varied leading to the different
408 outcomes we saw. Alternatively, we cannot rule out the possibility that SA treatment
409 activates responses not mediated by HRI that benefit viral replication.

410 In addition to inducing eIF2 α phosphorylation, SA induces the formation of stress
411 granules (SG). Consistent with the findings of Qin et al, we found that reovirus infection
412 induced SG formation early after infection with the number of SG reducing by 8 h and
413 disappearing late in infection. Our data in CV-1 cells are not consistent with the report by

414 Smith et al, who detected SGs at 19.5 h post-infection of DU145 cells [15, 16]. While it
415 is likely that different strains of reovirus induce SG to varying extents, and that this is
416 influenced by cell type and MOI, our data using the type 3 Dearing strain suggests that
417 infection with this strain of reovirus results in a low level of SG induction that is absent at
418 late times post infection. The timing of SG appearance (peak at 6 h) and dissolution
419 (beginning at 8 h) in our hands supports the idea put forth by Qin et al that SG induction
420 is linked to VF formation and that the onset of viral translation interferes with SG
421 stability [16]. Smith et al stained reovirus-infected cells at 19.5 h post-infection for the
422 SG protein, TIAR, but did not co-stain for a viral protein, such as μ NS, to detect viral
423 factories. We and others have observed that the SG protein G3BP1 localizes to the outer
424 margins of viral factories at late times post infection in a fraction of reovirus infected
425 cells [17]. Therefore, the TIAR-positive punctae seen at 19.5 h post-infection by Smith
426 may in fact have been viral factories that were co-staining for the presence of TIAR [15].
427 The significance of SG protein relocalization to VFs remains to be determined. Still,
428 these data imply that reovirus has evolved mechanisms to counter the cellular antiviral
429 activity of translation suppression through stress granule induction.

430 Pre-treatment of cells with SA led to enhanced viral protein expression, increased
431 infectivity, and higher viral titers. Given that reovirus compartmentalizes the translational
432 machinery in VF and that components of the translational machinery are also sequestered
433 within SGs, we previously speculated that SGs may serve as a reservoir of translational
434 machinery for reovirus VFs [23]. However, comparison of reovirus infection following
435 pre-treatment with either SA or heat shock (HS) suggests that the benefit is independent
436 of SG formation, as both treatments resulted in a robust induction of SGs, but only SA

437 pre-treatment led to an increase in viral replication. As we only examined viral
438 replication late during infection, it is possible that we missed early differences.
439 Additionally, since we were unable to achieve robust SG formation following HS in CV-
440 1 cells, viral replication studies were performed in L cells. Therefore, we can't rule out
441 cell-specific influences.

442 Our data is consistent with the findings of Smith et al that reovirus benefits from
443 activation of the ISR. In that study, the authors found that reovirus replicated to lower
444 titers in cells lacking a phosphorylatable eIF2 α [15]. SA is a potent activator of the ISR.
445 SA-mediated activation of the HRI kinase leads to phosphorylation of eIF2 α and
446 downstream upregulation of ATF4 and other transcriptional mediators of the ISR [27].
447 Given that canonical cap-dependent cellular translation relies on the availability of active
448 GTP.eIF2, it is possible that activation of the ISR allows reovirus mRNAs a competitive
449 advantage for limited translational machinery. The effect of SA was greatest when added
450 before reovirus adsorption but was still beneficial if treatment occurred within the first 4
451 h of infection. Translation of reovirus mRNAs rises sharply at ~ 6 h p.i. and peaks at ~12
452 h p.i. [30]. Given that the rising level of viral protein synthesis is concomitant with
453 continued host protein synthesis, it is possible that SA treatment selectively reduces the
454 translational machinery available for host protein synthesis [30]. It has been postulated
455 that heightened eIF2 α -phosphorylation may more strongly affect mRNAs containing
456 long or highly structured 5' untranslated regions (UTRs) [31, 32]. Reovirus mRNAs have
457 short 5' and 3' UTRs, possibly providing protection to viral mRNAs during translation
458 [33, 34]. Our findings that reovirus protein expression and infectivity were unaffected

459 when we treated cells with salubrinal to prevent de-phosphorylation of eIF2 α further
460 supports this and suggests that reovirus is refractory to salubrinal exposure.

461 It is known that under times of stress and reduced availability of active eIF2, cells
462 can utilize other initiation factors to ensure translation of select mRNAs. These factors,
463 including eIF2A, eIF2D, ligatin, MCT-1/DENR, and N-terminally truncated eIF5B₄₇₉₋₁₂₂₀,
464 can promote efficient recruitment of Met-tRNA^{Met}_i to the 40S/mRNA complex under
465 varying circumstances [35-39]. Several viruses take advantage of these alternative
466 initiation pathways including Sindbis virus and poliovirus [36, 39]. We have noted that
467 two of these factors, eIF2A and eIF5B localize to viral factories within infected cells
468 (unpublished observations, JSLP). As yet, we do not know if these factors play a
469 functional role in translation of viral mRNAs within VFs or if they are being sequestered
470 to prevent cellular mRNA translation.

471 We cannot exclude the possibility that pre-treatment of cells with SA has other
472 effects that promote viral replication independently of eIF2 α phosphorylation. Reovirus
473 is an oncolytic virus, preferentially infecting cancer cells. This phenomenon has been
474 linked to a mutationally-active Ras pathway, however reports have been conflicting
475 regarding Ras dependency [40-43]. Cancer cells have elevated levels of chaperones that
476 facilitate the high levels of protein synthesis typical of transformed cells. The efficiency
477 of mRNA translation is increased in the presence of supplemental recombinant Hsc70
478 and the rate of translation elongation may be regulated by chaperone availability [44].
479 Treatment with SA also increases Hsc70/Hsp70 chaperone levels in cells [45].
480 Furthermore, Hsc70 is required for HRI activation and blockade of Hsc70 disrupts HRI
481 activation [7]. We have previously reported that Hsc70 is specifically targeted to the viral

482 factory, although why this protein is specifically recruited remains unclear as its
483 recruitment is independent of its chaperone function [46]. It is conceivable that SA pre-
484 treatment could alter the availability of Hsc70 or other protein folding chaperones in a
485 way that is favorable during reovirus replication.

486 Infection with reovirus results in increased expression of stress response genes
487 including Hsc70, and GADD34, the latter of which complexes with protein phosphatase 1
488 to reverse eIF2 α phosphorylation. We observed that Type 3 Dearing (T3D) reovirus
489 protein expression was unaffected in the presence of salubrinal, a selective inhibitor of
490 the GADD34/PP1 α complex responsible for dephosphorylating eIF2 α , even in cells pre-
491 treated with SA to elevate the level of phosphorylated eIF2 α . The observation that
492 salubrinal was not anti-viral to T3D reovirus is not unique. Rotavirus, a fellow member of
493 the Reoviridae family, as well as other viruses including hepatitis C virus and mouse
494 hepatitis coronavirus, demonstrate continued viral protein synthesis despite heightened
495 eIF2 α -phosphorylation [47-49]. While this provides additional evidence that reovirus
496 benefits from the ISR, it is important to note that reovirus-induced expression of stress
497 response genes is not uniform and that host shutoff strains, including C8 and C87 (Type 3
498 Abney, T3A), induce increased expression of these genes compared to T3D, which is not
499 considered a host shutoff strain. While all reovirus strains tested, including T3A,
500 benefited from SA-pre-treatment, host shutoff strains may respond differently from T3D
501 to salubrinal treatment [15].

502 In addition to strain-specific differences in the ability to induce host shutoff, cell
503 differences have also been recorded. For instance, reovirus-induced host shutoff was not
504 observed in HeLa cells but was in L cells [30]. This may be linked to our observation that

505 T3D infection in HeLa cells is unaffected by SA pre-treatment, whereas SA pre-treatment
506 is beneficial in other cell types including L cells, CV-1 and HPDE cells.

507 Overall, this study finds that sodium arsenite-induced activation of the ISR prior
508 to reovirus inoculation results in enhanced viral protein expression, increased infectivity
509 and higher viral yield. Furthermore, HRI kinase activation of the ISR is insufficient for
510 replication enhancement as both heat shock and sodium arsenite activate the HRI kinase,
511 but only sodium arsenite treatment was associated with increased viral infectivity and
512 higher yield. Finally, sodium arsenite-induced enhancement was observed across reovirus
513 strains but was not observed in all cell types suggesting a role for cell-type-specific
514 influences. Understanding the interplay between reovirus and the ISR, and how to
515 modulate it to enhance virus replication, could reveal novel targets to strengthen the
516 oncolytic potential of reovirus.

517

518

519

520

521

522

523

524

525

526

527

528 **ACKNOWLEDGEMENTS**

529 Work in E.D.L.'s lab was supported by Le Moyne College Research and Development

530 Grants (to E.D.L), and Le Moyne College Student Research Grants awarded to M.M.L

531 and M.P.W..

532

533

534

535

536

537

538

539

540

541

542

543

544

545

546

547

548

549

550

551 **REFERENCES**

552

- 553 1. Garcia MA, Meurs EF, Esteban M: **The dsRNA protein kinase PKR: virus**
554 **and cell control.** *Biochimie* 2007, **89**(6-7):799-811.
- 555 2. Berlanga JJ, Ventoso I, Harding HP, Deng J, Ron D, Sonenberg N, Carrasco L, de
556 Haro C: **Antiviral effect of the mammalian translation initiation factor**
557 **2alpha kinase GCN2 against RNA viruses.** *EMBO J* 2006, **25**(8):1730-1740.
- 558 3. Cheng G, Feng Z, He B: **Herpes simplex virus 1 infection activates the**
559 **endoplasmic reticulum resident kinase PERK and mediates eIF-2alpha**
560 **dephosphorylation by the gamma(1)34.5 protein.** *J Virol* 2005,
561 **79**(3):1379-1388.
- 562 4. Pakos-Zebrucka K, Koryga I, Mnich K, Ljujic M, Samali A, Gorman AM: **The**
563 **integrated stress response.** *EMBO Rep* 2016, **17**(10):1374-1395.
- 564 5. Hamanaka RB, Bennett BS, Cullinan SB, Diehl JA: **PERK and GCN2**
565 **contribute to eIF2alpha phosphorylation and cell cycle arrest after**
566 **activation of the unfolded protein response pathway.** *Mol Biol Cell* 2005,
567 **16**(12):5493-5501.
- 568 6. Harding HP, Zhang Y, Zeng H, Novoa I, Lu PD, Calton M, Sadri N, Yun C, Popko
569 B, Paules R *et al*: **An integrated stress response regulates amino acid**
570 **metabolism and resistance to oxidative stress.** *Mol Cell* 2003, **11**(3):619-
571 633.
- 572 7. Lu L, Han AP, Chen JJ: **Translation initiation control by heme-regulated**
573 **eukaryotic initiation factor 2alpha kinase in erythroid cells under**
574 **cytoplasmic stresses.** *Mol Cell Biol* 2001, **21**(23):7971-7980.
- 575 8. Anda S, Zach R, Grallert B: **Activation of Gcn2 in response to different**
576 **stresses.** *PLoS One* 2017, **12**(8):e0182143.
- 577 9. Pyo CW, Lee SH, Choi SY: **Oxidative stress induces PKR-dependent**
578 **apoptosis via IFN-gamma activation signaling in Jurkat T cells.** *Biochem*
579 *Biophys Res Commun* 2008, **377**(3):1001-1006.
- 580 10. Kedersha NL, Gupta M, Li W, Miller I, Anderson P: **RNA-binding proteins**
581 **TIA-1 and TIAR link the phosphorylation of eIF-2 alpha to the assembly**
582 **of mammalian stress granules.** *J Cell Biol* 1999, **147**(7):1431-1442.
- 583 11. Tourriere H, Chebli K, Zekri L, Courselaud B, Blanchard JM, Bertrand E, Tazi J:
584 **The RasGAP-associated endoribonuclease G3BP assembles stress**
585 **granules.** *J Cell Biol* 2003, **160**(6):823-831.
- 586 12. Dauber B, Wolff T: **Activation of the Antiviral Kinase PKR and Viral**
587 **Countermeasures.** *Viruses* 2009, **1**(3):523-544.
- 588 13. Krishnamoorthy J, Mounir Z, Raven JF, Koromilas AE: **The eIF2alpha**
589 **kinases inhibit vesicular stomatitis virus replication independently of**
590 **eIF2alpha phosphorylation.** *Cell Cycle* 2008, **7**(15):2346-2351.
- 591 14. Smith JA, Schmechel SC, Williams BR, Silverman RH, Schiff LA: **Involvement**
592 **of the interferon-regulated antiviral proteins PKR and RNase L in**
593 **reovirus-induced shutoff of cellular translation.** *J Virol* 2005, **79**(4):2240-
594 2250.

- 595 15. Smith JA, Schmechel SC, Raghavan A, Abelson M, Reilly C, Katze MG, Kaufman
596 RJ, Bohjanen PR, Schiff LA: **Reovirus induces and benefits from an**
597 **integrated cellular stress response.** *J Virol* 2006, **80**(4):2019-2033.
- 598 16. Qin Q, Hastings C, Miller CL: **Mammalian orthoreovirus particles induce**
599 **and are recruited into stress granules at early times postinfection.** *J*
600 *Virol* 2009, **83**(21):11090-11101.
- 601 17. Choudhury P, Bussiere L, Miller CL: **Mammalian Orthoreovirus Factories**
602 **Modulate Stress Granule Protein Localization by Interaction with**
603 **G3BP1.** *J Virol* 2017.
- 604 18. Becker MM, Peters TR, Dermody TS: **Reovirus sigma NS and mu NS**
605 **proteins form cytoplasmic inclusion structures in the absence of viral**
606 **infection.** *J Virol* 2003, **77**(10):5948-5963.
- 607 19. Goral MI, Mochow-Grundy M, Dermody TS: **Sequence diversity within the**
608 **reovirus S3 gene: reoviruses evolve independently of host species,**
609 **geographic locale, and date of isolation.** *Virology* 1996, **216**(1):265-271.
- 610 20. Virgin HWT, Bassel-Duby R, Fields BN, Tyler KL: **Antibody protects against**
611 **lethal infection with the neurally spreading reovirus type 3 (Dearing).** *J*
612 *Virol* 1988, **62**(12):4594-4604.
- 613 21. Fields BN, Raine CS, Baum SG: **Temperature-sensitive mutants of reovirus**
614 **type 3: defects in viral maturation as studied by immunofluorescence**
615 **and electron microscopy.** *Virology* 1971, **43**(3):569-578.
- 616 22. Miller CL, Arnold MM, Broering TJ, Hastings CE, Nibert ML: **Localization of**
617 **mammalian orthoreovirus proteins to cytoplasmic factory-like**
618 **structures via nonoverlapping regions of microNS.** *J Virol* 2010,
619 **84**(2):867-882.
- 620 23. Desmet EA, Anguish LJ, Parker JS: **Virus-mediated compartmentalization**
621 **of the host translational machinery.** *MBio* 2014, **5**(5):e01463-01414.
- 622 24. Reineke LC, Lloyd RE: **Diversion of stress granules and P-bodies during**
623 **viral infection.** *Virology* 2013, **436**(2):255-267.
- 624 25. Broering TJ, Parker JS, Joyce PL, Kim J, Nibert ML: **Mammalian reovirus**
625 **nonstructural protein microNS forms large inclusions and colocalizes**
626 **with reovirus microtubule-associated protein micro2 in transfected**
627 **cells.** *J Virol* 2002, **76**(16):8285-8297.
- 628 26. Qin Q, Carroll K, Hastings C, Miller CL: **Mammalian orthoreovirus escape**
629 **from host translational shutoff correlates with stress granule**
630 **disruption and is independent of eIF2alpha phosphorylation and PKR.** *J*
631 *Virol* 2011, **85**(17):8798-8810.
- 632 27. McEwen E, Kedersha N, Song B, Scheuner D, Gilks N, Han A, Chen JJ, Anderson
633 P, Kaufman RJ: **Heme-regulated inhibitor kinase-mediated**
634 **phosphorylation of eukaryotic translation initiation factor 2 inhibits**
635 **translation, induces stress granule formation, and mediates survival**
636 **upon arsenite exposure.** *J Biol Chem* 2005, **280**(17):16925-16933.
- 637 28. Novoa I, Zeng H, Harding HP, Ron D: **Feedback inhibition of the unfolded**
638 **protein response by GADD34-mediated dephosphorylation of**
639 **eIF2alpha.** *J Cell Biol* 2001, **153**(5):1011-1022.

- 640 29. Boyce M, Bryant KF, Jousse C, Long K, Harding HP, Scheuner D, Kaufman RJ,
641 Ma D, Coen DM, Ron D *et al*: **A selective inhibitor of eIF2alpha**
642 **dephosphorylation protects cells from ER stress.** *Science* 2005,
643 **307**(5711):935-939.
- 644 30. Munoz A, Alonso MA, Carrasco L: **The regulation of translation in**
645 **reovirus-infected cells.** *J Gen Virol* 1985, **66 (Pt 10)**:2161-2170.
- 646 31. Mignone F, Gissi C, Liuni S, Pesole G: **Untranslated regions of mRNAs.**
647 *Genome Biol* 2002, **3**(3):REVIEWS0004.
- 648 32. Burwick N, Aktas BH: **The eIF2-alpha kinase HRI: a potential target**
649 **beyond the red blood cell.** *Expert Opin Ther Targets* 2017, **21**(12):1171-
650 1177.
- 651 33. Kozak M, Shatkin AJ: **Sequences and properties of two ribosome binding**
652 **sites from the small size class of reovirus messenger RNA.** *J Biol Chem*
653 1977, **252**(19):6895-6908.
- 654 34. Kozak M, Shatkin AJ: **Identification of features in 5' terminal fragments**
655 **from reovirus mRNA which are important for ribosome binding.** *Cell*
656 1978, **13**(1):201-212.
- 657 35. Dmitriev SE, Terenin IM, Andreev DE, Ivanov PA, Dunaevsky JE, Merrick WC,
658 Shatsky IN: **GTP-independent tRNA delivery to the ribosomal P-site by a**
659 **novel eukaryotic translation factor.** *J Biol Chem* 2010, **285**(35):26779-
660 26787.
- 661 36. Skabkin MA, Skabkina OV, Dhote V, Komar AA, Hellen CU, Pestova TV:
662 **Activities of Ligatin and MCT-1/DENR in eukaryotic translation**
663 **initiation and ribosomal recycling.** *Genes Dev* 2010, **24**(16):1787-1801.
- 664 37. Terenin IM, Dmitriev SE, Andreev DE, Shatsky IN: **Eukaryotic translation**
665 **initiation machinery can operate in a bacterial-like mode without eIF2.**
666 *Nat Struct Mol Biol* 2008, **15**(8):836-841.
- 667 38. Gonzalez-Almela E, Williams H, Sanz MA, Carrasco L: **The Initiation Factors**
668 **eIF2, eIF2A, eIF2D, eIF4A, and eIF4G Are Not Involved in Translation**
669 **Driven by Hepatitis C Virus IRES in Human Cells.** *Front Microbiol* 2018,
670 **9**:207.
- 671 39. White JP, Reineke LC, Lloyd RE: **Poliovirus switches to an eIF2-**
672 **independent mode of translation during infection.** *J Virol* 2011,
673 **85**(17):8884-8893.
- 674 40. Strong JE, Coffey MC, Tang D, Sabinin P, Lee PW: **The molecular basis of**
675 **viral oncolysis: usurpation of the Ras signaling pathway by reovirus.**
676 *EMBO J* 1998, **17**(12):3351-3362.
- 677 41. Marcato P, Shmulevitz M, Pan D, Stoltz D, Lee PW: **Ras transformation**
678 **mediates reovirus oncolysis by enhancing virus uncoating, particle**
679 **infectivity, and apoptosis-dependent release.** *Mol Ther* 2007, **15**(8):1522-
680 1530.
- 681 42. Rudd P, Lemay G: **Correlation between interferon sensitivity of reovirus**
682 **isolates and ability to discriminate between normal and Ras-**
683 **transformed cells.** *J Gen Virol* 2005, **86**(Pt 5):1489-1497.

- 684 43. Song L, Ohnuma T, Gelman IH, Holland JF: **Reovirus infection of cancer**
685 **cells is not due to activated Ras pathway.** *Cancer Gene Ther* 2009,
686 **16(4):382.**
- 687 44. Liu B, Han Y, Qian SB: **Cotranslational response to proteotoxic stress by**
688 **elongation pausing of ribosomes.** *Mol Cell* 2013, **49(3):453-463.**
- 689 45. Somji S, Todd JH, Sens MA, Garrett SH, Sens DA: **Expression of the**
690 **constitutive and inducible forms of heat shock protein 70 in human**
691 **proximal tubule cells exposed to heat, sodium arsenite, and CdCl(2).**
692 *Environ Health Perspect* 1999, **107(11):887-893.**
- 693 46. Kaufer S, Coffey CM, Parker JS: **The cellular chaperone hsc70 is**
694 **specifically recruited to reovirus viral factories independently of its**
695 **chaperone function.** *J Virol* 2012, **86(2):1079-1089.**
- 696 47. Garaigorta U, Chisari FV: **Hepatitis C virus blocks interferon effector**
697 **function by inducing protein kinase R phosphorylation.** *Cell Host Microbe*
698 2009, **6(6):513-522.**
- 699 48. Rojas M, Arias CF, Lopez S: **Protein kinase R is responsible for the**
700 **phosphorylation of eIF2alpha in rotavirus infection.** *J Virol* 2010,
701 **84(20):10457-10466.**
- 702 49. Raaben M, Groot Koerkamp MJ, Rottier PJ, de Haan CA: **Mouse hepatitis**
703 **coronavirus replication induces host translational shutoff and mRNA**
704 **decay, with concomitant formation of stress granules and processing**
705 **bodies.** *Cell Microbiol* 2007, **9(9):2218-2229.**
706

707

708

709

710

711

712

713

714

715

716

717

718 **FIGURE LEGENDS**

719 **Figure 1. Reovirus infection induces the formation of stress granules at early times**

720 **post infection.** (A) CV-1 cells were mock infected, pre-treated with 0.5 mM sodium

721 arsenite (SA) for 30 min, or infected with T3D at an MOI = 10. At the indicated times,

722 cells were fixed and co-immunostained for G3BP (red) and TIAR (green), upper panels,

723 to detect stress granules (SG) in uninfected cells or TIAR (green) and μ NS (red), lower

724 panels, to detect SG in T3D-infected cells. Cell nuclei were stained with DAPI (blue).

725 Mock and SA-treated cells were fixed at 0 h. (B) The percent cells containing SG from

726 panel A was quantified [$(\# \text{ of cells containing SG} / \text{total } \# \text{ of cells}) \times 100$] from a

727 minimum of three independent experiments. ** $P < 0.01$, **** $P < 0.0001$; two-tailed

728 unpaired t test. (C) CV-1 cells were infected with T3D at an MOI = 0.5 and at 8 and 24 h

729 p.i. cells were fixed and co-immunostained with G3BP (green) and μ NS (red), upper

730 panels. Alternatively, CV-1 cells were infected with T3D at an MOI = 1 and at 23.5 h

731 cells were post-treated with 0.5 mM SA for 30 min. At 24 h p.i. cells were fixed and co-

732 immunostained with G3BP (green) and μ NS (red), lower panels. (D) Mock infected (-)

733 or T3D infected cells were lysed at 2 or 18 h p.i and the expression level of the indicated

734 proteins was determined by immunoblotting.

735

736 **Figure 2. Pre-treatment with 0.5 mM sodium arsenite enhances reovirus infectivity.**

737 (A) CV-1 cells were mock infected or infected with T3D at an MOI = 1. Cells were left

738 untreated (-), treated with 0.5 mM SA for 30 min prior to infection (pre) or were treated

739 with 0.5 mM SA for 30 min immediately before lysis (post). At the indicated time points,

740 cells were harvested and protein expression was determined by immunoblot. (B) CV-1

741 cells were infected with T3D at an MOI = 1. Cells were left untreated or treated with 0.5
742 mM SA for 30 min prior to infection (pre). At 18 h p.i., cells were fixed and
743 immunostained with for μ NS (red) and DAPI (nuclei, blue). (C) The percent cells
744 containing viral factories (VF) as represented in panel B was quantified [(# of cells
745 containing VF / total # of cells) \times 100] from three independent experiments. (D) CV-1
746 cells were left untreated or were pre-treated with 0.5 mM SA for 30 min prior to infection
747 with T3D at the indicated an MOI. At 18 h p.i., cells were subjected to the standard MRV
748 plaque assay in L929 cells and plaques were counted from at least three independent
749 experiments. * $P < 0.05$, ** $P < 0.01$, **** $P < 0.0001$; two-tailed unpaired t test.

750

751 **Figure 3. Pre-treatment with 0.5 mM sodium arsenite enhances permissivity in a**
752 **cell-type-specific manner across reovirus strains.** (A) CV-1, HeLa, L929 or HPDE
753 cells were left untreated (No SA) or were treated with 0.5 mM SA for 30 min prior to
754 infection (Pre-SA). Following this, cells were infected with T3D at an MOI = 1. At 18 h
755 p.i., cells were fixed and immunostained for μ NS (red) and DAPI (nuclei, blue). The
756 percent of cells containing viral factories (VF) was quantified [(# of cells containing VF /
757 total # of cells) \times 100] from three independent experiments. (B) CV-1 cells were left
758 untreated (No SA) or were treated with 0.5 mM SA prior to infection (Pre-SA). Cells
759 were then infected with reovirus strains T3D, T1L, or T3A such that ~20% of cells were
760 infected. At 18 h p.i., cells were fixed and immunostained for μ NS (red) and DAPI
761 (nuclei, blue). The percent of cells containing VF was quantified [(# of cells containing
762 VF / total # of cells) \times 100] from three independent experiments. * $P < 0.05$; ** $P <$
763 0.01; two-tailed unpaired t test.

764

765 **Figure 4. Heat shock enhances reovirus-protein expression, but not infectivity, in**
766 **L929 cells.** (A) L929 cells were left untreated (unt), were pre-treated with 0.5 mM SA
767 (SA) or were heat shocked at 44°C for 45 min (HS) before fixing and immunostaining for
768 G3BP (green) to detect stress granules (SG). The percentage of SG induced was
769 quantified [(# of cells containing SG / total # of cells) × 100] from three independent
770 experiments. (B) L929 cells were left untreated or were heat shocked as above
771 immediately prior to infection with T3D at an MOI = 1. At the indicated time points,
772 cells were lysed and the expression levels of the indicated proteins was determined by
773 immunoblot. (C) L929 cells were left untreated, treated with 0.5 mM SA for 30 min or
774 were heat shocked as above. Following this, cells were infected with T3D at an MOI = 1.
775 At 18 h p.i, cells were fixed and immunostained for μNS (red) and DAPI (nuclei, blue).
776 (D) The percent cells containing viral factories (VF) as represented in panel C was
777 quantified [(# of cells containing VF / total # of cells) × 100] from at least three
778 independent experiments. (E) L929 cells were left untreated or were heat shocked as
779 above prior to infecting with T3D at an MOI = 1. At 18 h p.i., cells were subjected to the
780 standard MRV plaque assay in L929 cells and plaques were counted from at least three
781 independent experiments. *** $P < 0.001$; two-tailed unpaired t test.

782

783 **Figure 5. Addition of sodium arsenite prior to 4 h p.i. enhances reovirus**
784 **permissivity.** CV-1 cells were left untreated (Unt), were pre-treated with 0.5 mM SA for
785 30 min prior to virus inoculation (pre-SA) or were treated with 0.5 mM SA for 30 min at
786 the indicated times post infection. At 18 h p.i., cells were fixed and immunostained for

787 μ NS (red) and DAPI (nuclei, blue). (B) Representative images from each of the
788 conditions above. The percent cells containing viral factories (VF) was quantified [(# of
789 cells containing VF / total # of cells) \times 100] from four independent experiments. ** $P <$
790 0.01; *** $P <$ 0.001; n.s. denotes not significant; two-tailed unpaired t test.

791

792 **Figure 6. Salubrinal treatment does not negatively impact reovirus infection.** (A)

793 CV-1 cells were left untreated (-), were pre-treated with 0.5 mM SA for 30 min (SA) or
794 were infected with T3D at an MOI = 10 in the presence or absence of SA pre-treatment.
795 Immediately following infection, salubrinal (Sal) was added to T3D-infected cells at the
796 indicated concentrations. At 18 h p.i., cells were lysed and the expression levels of the
797 indicated proteins were determined by immunoblot. (B) CV-1 cells were left untreated or
798 treated with 0.5 mM SA for 30 min prior to infection with T3D at an MOI = 1. Following
799 infection, 50 mM salubrinal was added where indicated. At 18 h p.i., cells were fixed and
800 immunostained for μ NS (red) and DAPI (nuclei, blue). (C) The percent cells containing
801 viral factories (VF) as represented in panel B was quantified [(# of cells containing VF /
802 total # of cells) \times 100] from 3 independent experiments. * $P <$ 0.05, ** $P <$ 0.01; two-
803 tailed unpaired t test.

804

FIGURE 1

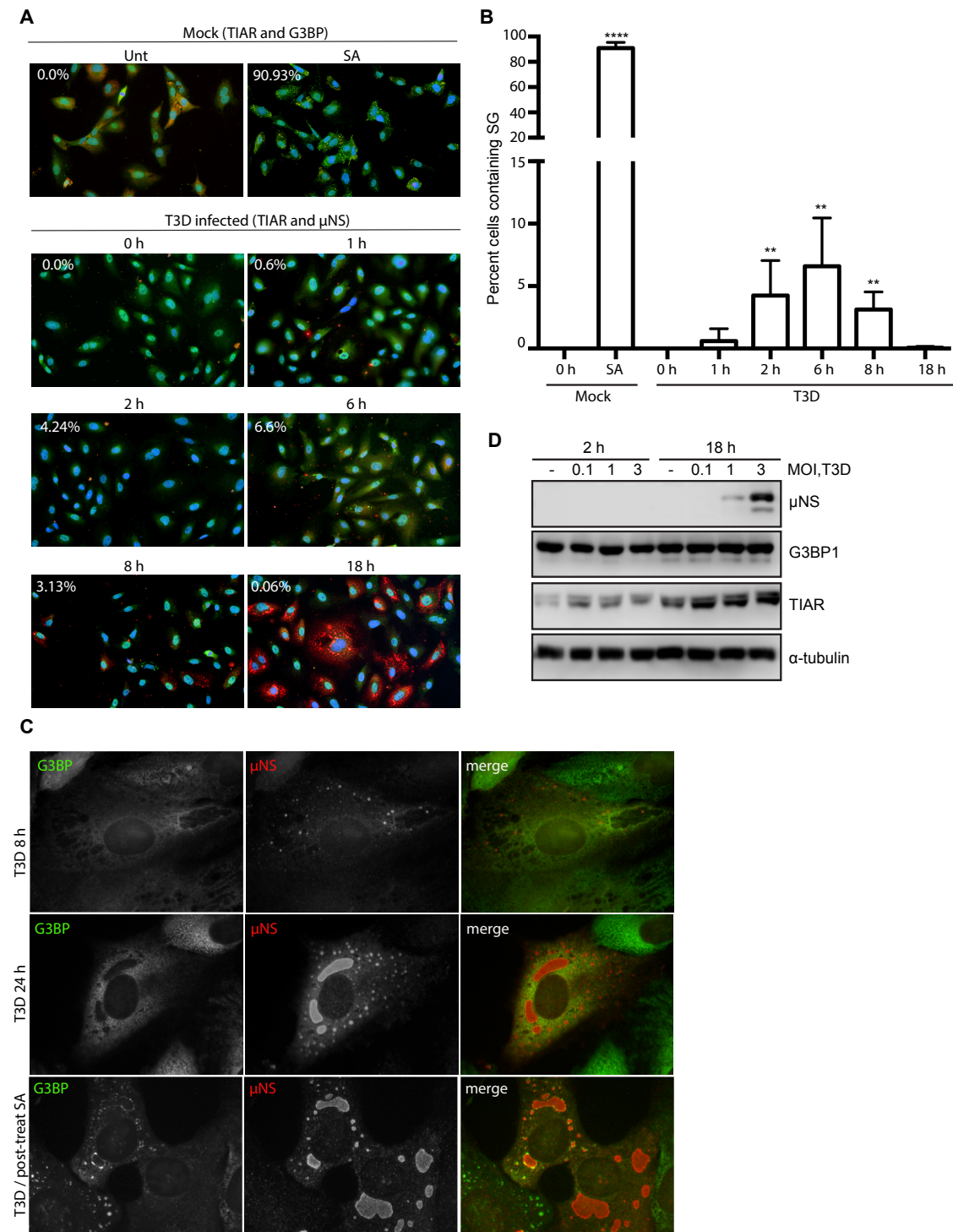


FIGURE 2

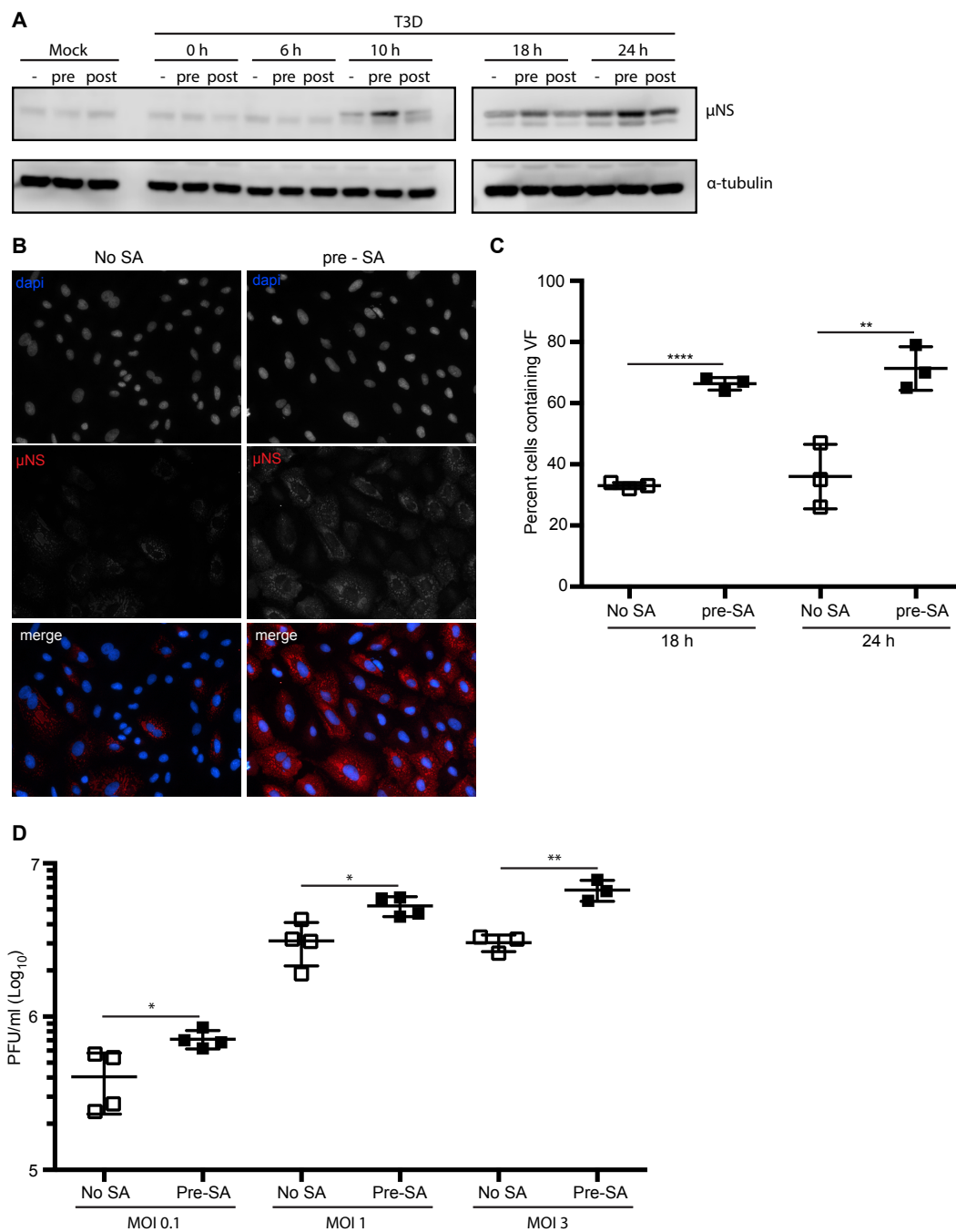


FIGURE 3

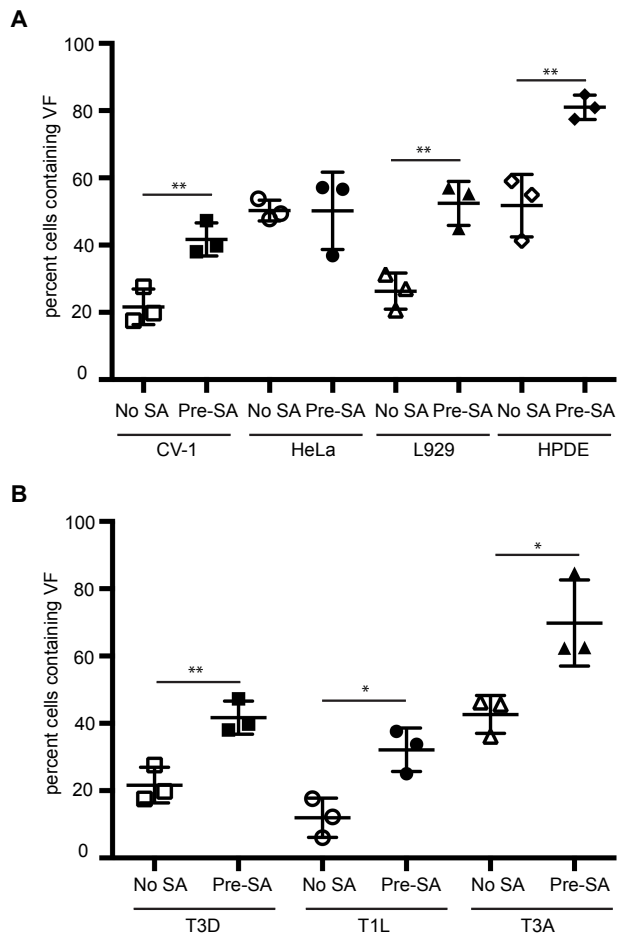


FIGURE 4

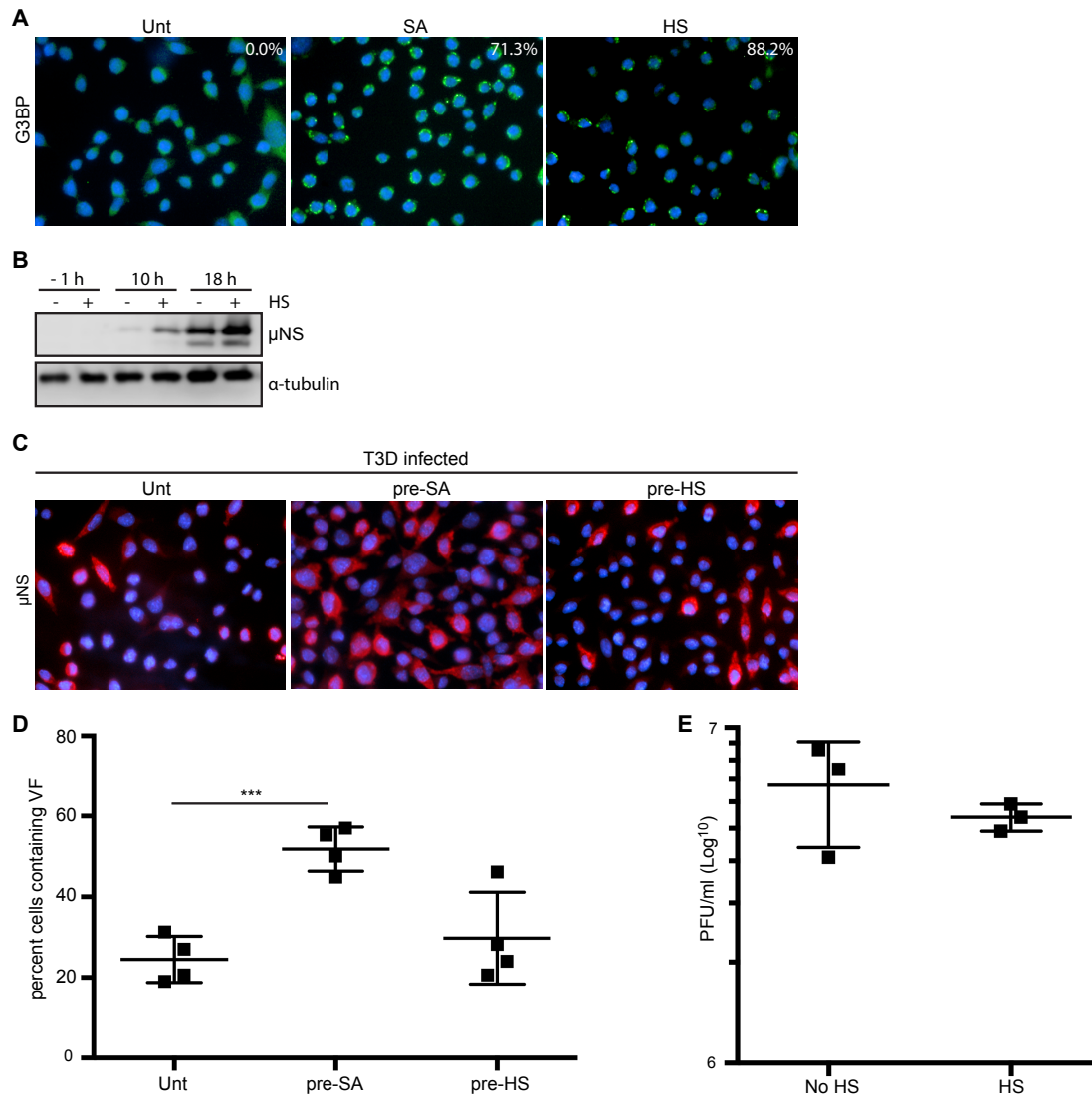


FIGURE 5

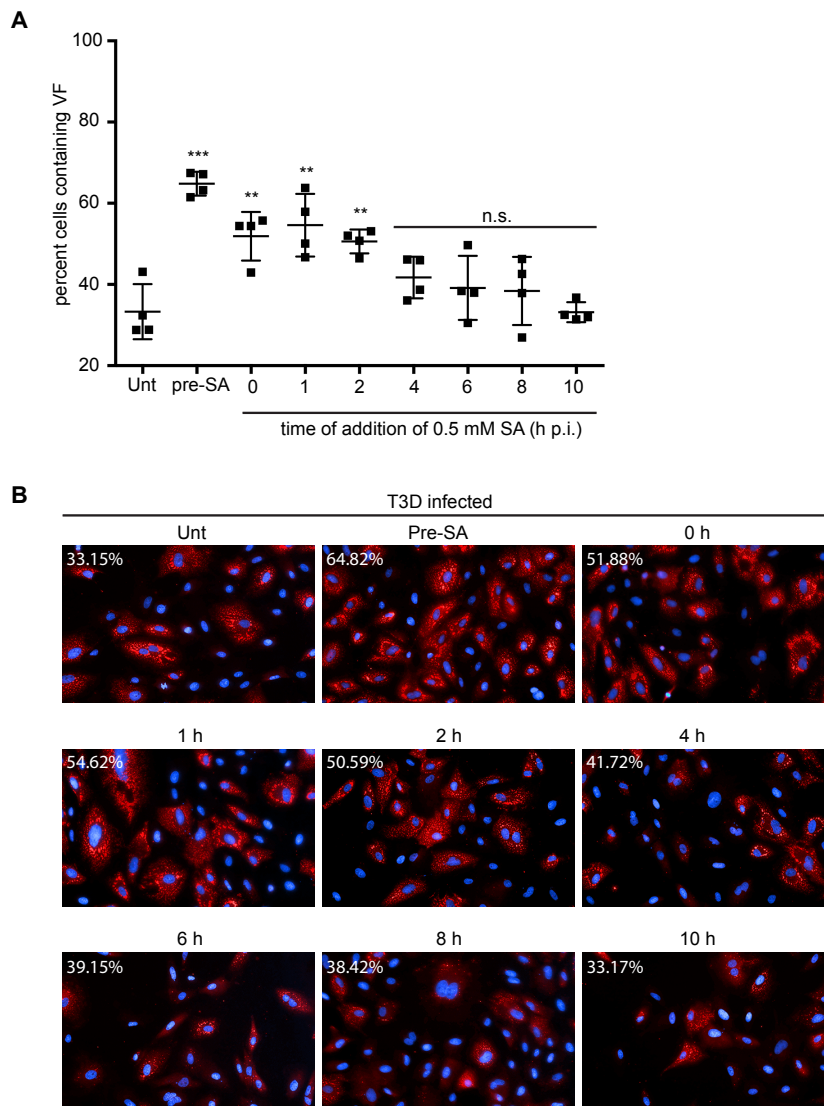


FIGURE 6

